Radiation-induced graft polymerization of N-isopropyl acrylamide onto microcrystalline cellulose: Assessing the efficiency of the peroxidation method

Siti Fatahiyah Mohamad, Véronique Aguié-Béghin, Bernard Kurek, Xavier X. Coqueret

Version of Record: https://www.sciencedirect.com/science/article/pii/S0969806X22000809
Manuscript_750fa4764f864113963fb99df27a4cf3

Radiation-induced graft polymerization of N-isopropyl acrylamide onto microcrystalline cellulose: assessing the efficiency of the peroxidation method

Siti Fatahiyah Mohamad[a,b,c], Véronique Aguié-Béghin[b], Bernard Kurek[b] and Xavier Coqueret[a]

[a] Université de Reims Champagne-Ardenne, CNRS UMR 7312, Institut de Chimie Moléculaire de Reims, BP 1039, 51687 Reims, France

[b] Université de Reims Champagne-Ardenne, INRAE, FARE, UMR A 614, 51097 Reims, France

[c] Radiation Processing and Technology, Malaysia Nuclear Agency,41300 Bangi Selangor, Malaysia

Corresponding authors: fatahiyah@nuclearmalaysia.gov.my, xavier.coqueret@univ-reims.fr

Abstract

This article reports on the development of an experimental protocol based on the radiation-induced graft polymerization of a temperature-responsive polymer onto cellulose (MCC). MCC was selected as a model substrate, in view of modifying cellulose nanocrystals (CNCs). Two different grafting methods, by pre-irradiation or simultaneous procedure, were performed to assess their efficiency and identify key experimental steps. The Fenton reaction was successfully applied to radiation-peroxidized MCC. The effects of radiation dose, reaction temperature, monomer concentration and reaction time were studied in various combinations to control the polymerization of N-isopropyl acrylamide (NIPAM). The amount of poly(NIPAM) grafted on MCC was determined by elemental analysis. Grafted MCC samples were characterized by infrared spectroscopy, thermogravimetry, scanning electron microscopy and X-ray diffraction to compare their features with the unmodified substrate. This experimental approach was then applied to CNCs. The grafting and purification protocols for the modified CNCs were adapted accordingly. Preliminary characterization shows the presence of the poly(NIPAM) grafts onto the CNCs and evidences the temperature-reponsiveness of the obtained material.

Keywords

Radiation-induced graft polymerization - Microcrystalline cellulose - Cellulose nanocrystals – Poly(N-isopropyl acrylamide) - Temperature-responsive nanoparticles

Highlights

• Radiation-induced peroxidation of cellulose is a simple method for graft-polymerization

• Grafting of NIPAM onto peroxidized MCC and CNC is achieved at RT in presence of Fe(II)

• Experimental conditions can be adjusted to exert a control on the extent of grafting

• The protocol based on Fenton reaction is well adapted for grafting polymers with LCST > RT

• Temperature-responsive poly(NIPAM) grafts on CNCs are evidenced by turbidimetry

Introduction

The objective of the work reported in this article was to develop a robust protocol for the radiation-induced graft polymerization of N-isopropyl acrylamide, using microcrystalline cellulose (MCC) as a model starting material. The final goal is the controlled modification of cellulose nanocrystals (CNCs) by grafting a temperature-responsive hydrophilic polymer, poly(N-isopropyl acrylamide). Manipulation of CNCs maintained in an unaggregated state requires specific and complex procedures. There was a need for a robust protocol before facing the specific aspects of CNC activation and /or polymerization mediated by radiation treatment and the subsequent stages for isolation and purification of the resulting nanomaterials.

The surface functionalization of cellulose-based substrates via radiation-induced graft polymerization (RIGP) has been identified very early as a clean and efficient method to enhance or to impart new properties to various types of bio-based materials treated in many different physical forms (powders, fibres and fabrics, pulp and paper, films and membranes, molded thermoplastics, ...) (Chapiro, 1962). Since the very early reports on RIGP, the basic understanding has been gradually enhanced while methodologic improvements have been made available to exert a better controll over the procedures. Technical and environmental

advantages (Guthrie, 1974 ; Garnett, 1979; Stannett, 1990; Wojnárovits et al., 2010) as well as potential economic benefits (Aoki et al., 2013) continue to arouse much attention from academic and industrial researchers. Radiation processing is indeed particularly suited for activating polymers *via* the generation of free radicals which can initiate polymerization from activated or activable "trunk" polymers according to one of the following processes.

Basically, three synthetic approaches mediated by high energy radiation can lead to free radical graft polymerization (Nasef and Güven, 2012; Bhardwaj et al., 2014). The main differences between these methods arise both from the chemical transformation induced during the irradiation stage and the composition of the medium surrounding the substrate to be grafted. In pathway (a) of Scheme 1, the selected radiation, most commonly gamma radiation and electron beam (EB), interact simultaneously with the substrate and the surrounding medium which contains the monomer. This results in the mutual grafting of the two components. The pre-irradiation method (pathway b) consists in irradiating the substrate in vacuum or an inert atmosphere followed by immediate or delayed immersion into a monomer solution or in pure liquid monomer. In the variant based on peroxidation (pathway c), pre-irradiation is conducted in the presence of oxygen, generally in air, or in oxygenated media, to convert free radicals formed in zones in contact with oxygen into peroxides and hydroperoxides (Şolpan et al., 2010). This provides a simple route to generate polymer-bound initiators which can be decomposed on command by thermal activation or by reaction with appropriate reductive agent to trigger the graft polymerization under inert conditions. Free radical formed in crystalline domains may persist for long periods within the irradiated material. These trapped free radicals can contribute to the delayed initiation of polymerization by thermal activation or by solvent diffusion, both factors having a positive effect on the mobility of monomer towards active centers, and *vice versa*.

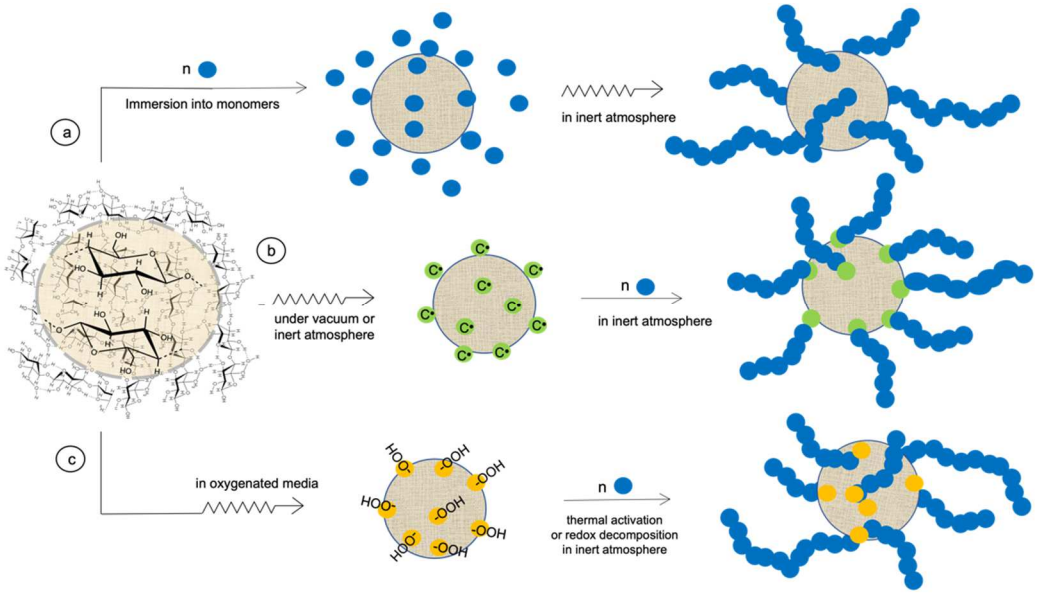

Scheme 1. Sketch representing the three basic graft polymerization methods onto MCC, using high energy radiation: simultaneous or mutual grafting method (a), and pre-irradiation methods with generation of long-lived C-centered free radicals in an inert atmosphere (b) and peroxidation in oxygenated media (c).

These three methods present specific advantages and drawbacks which have to be considered for selecting the best option. However, they are all subject to the same constraint of minimizing the radiation dose to preserve the basic properties of the substrate by limiting the scission of cellulose chains (Ershov, 1998; Takacs et al., 1999; Iller et al., 2002). The pre-irradiation method is preferred when it is advantageous to implement separately, in time and/or space, the radiation activation from the grafting stage. Active centers generated within the substrate can be stored for rather long periods of time by storage at low temperature. Peroxidation is relatively simpler to achieve since it does not require high-vacuum operations or deoxygenation and conditioning of the substrate with the use of inert gases.

Recent advances in this domain include the introduction of controlled free radical polymerization as a new approach of radiation- mediated grafting processes (Barsbay et al. 2007; Barsbay and Güven, 2019), the development of the concept of admicellar polymerization (Ulman and Shukla, 2015) and the application of RIGP to nanomaterials, such

as track-etched membranes with grafted nanopores (Clochard, et al., 2010) and surface-grafted nanoparticles (Kumar et a., 2014; Fu et al., 2020; Güven, 2021).

From a technological perspective, RIGP methods have been adapted to upgrade cotton and more generally cellulose-based textiles (Shahid-ul-Islam and Faqeer, 2015), or to elaborate natural fibers and fabrics possessing retention properties for various types of pollutants or industrial by-products, in view of environmental applications or recycling (Seko et al. 2005; Sharif et al., 2013; Othman et al., 2019). Radiation-induced graft polymerization (Bhattacharya and Misra, 2004) has also been considered as a method to modify natural fibres with various types of functionalities or graft polymers improving the performance of composite materials associating theses upgraded fibers with thermoplastics ot thermosets (Rodriguez et al., 1979; LeMoigne et al., 2017; Tataru et al., 2020). The modification of microcrystalline cellulose (MCC) has been achieved by mutual grafting of monomers in conventional organic solvents (Madrid and Abad, 2015) and in ionic liquids (Hao et al., 2009). However, this method is known to induce the formation of homopolymer and, more problematically, suffers from a lack of spatial control over the locus of initiation, while our ultimate goal is to modifiy the surface of CNCs with a LCST polymer, to confer switchable hydrophilicity to the grafted nanoparticles.

This is why we have explored in this study the peroxidation pathway, using MCC as an easy to handle substrate to evaluate more specifically the possibility to induce NIPAM polymerization by a Fenton reaction under various experimental conditions including pre-irradiation dose, NIPAM concentration and temperature of the grafting medium. Particular attention was paid to the impact of radiation on the crystalline structure of MCC and on the effect of temperature of the graft polymerization stage, since the extent of grafting process and the resulting morphology might be affected by the solution properties of the grafted chains.

Experimental part

Materials

The cellulosic substrate was purified microcrystalline cellulose (MCC) known as Avicel PH101 and commercialized by Sigma Aldrich, France. It was used in its original form, a white powder with an average particle size *ca.* 50 µm. Commercial poly (N-isopropyl acrylamide) with a number-average molecular weight approximately 40 000 was purchased from Sigma Aldrich France. N-isopropyl acrylamide and Mohr's salt (ferrous ammonium sulfate hexahydrate) were reagent grade chemicals from Alfa Aesar, France.

To test the grafting protocol on nanocellulose materials, CNCs were prepared and isolated from ramie fibers. The starting raw fibers were bleached and submitted to sulfuric acid-catalyzed hydrolysis according to the method described previously (Hambardzumyan et al., 2012). After repeated purification, CNCs were obtained as an aqueous suspension with a solid mass content 2.45 wt-%.

Irradiation of Cellulose Starting Materials

Electron beam irradiations were performed at Ionisos (Chaumesnil, France) using a 10 MeV, 33 kW Linac accelerator at a time-average dose rate of 15 kGy s^{-1}. Samples were treated at doses ranging from 10 to 50 kGy, in one or two passes, so as a single pass does not exceed 25 kGy to limit undesirable effects due to the raise in temperature during the treatment. Simultaneous grafting experiments were carried out on test tubes containing the desired amount of MCC (0.5 g) with 25 mL of NIPAM aqueous solution (0.1, 0.5 or 1 M). The tubes were thoroughly deaerated by flushing Ar for 30 min and closed with a septum under Ar flow before irradiation.

Peroxidation pretreatments were applied to MCC samples sealed into plastic bags in presence of air (10 g per sample bag). CNC samples were irradiated as aqueous suspensions of the

purified nanoparticles diluted to reach a concentration of 1 wt-%. The solutions were conditioned by 10 mL volume units poured into 25 mL Pyrex test tubes tightly closed in the presence of air. The test tubes were irradiated at 50 kGy (2 passes of 25 kGy). Irradiated samples were stored at -50°C and reconditioned at RT about 2 h before starting the grafting reaction.

Graft polymerization on peroxidized cellulose

In a typical experiment, a stock solution (75-80 mL) of NIPAM (from 0.1 M to 1.0 M) with 0.4 mM of Mohr's salt in deionized water was prepared and in poured into a 100 mL-cylinder. The cylinder was purged with gaseous nitrogen for 15 minutes to eliminate oxygen before use. A sample of irradiated MCC (0.5 g) was placed in a closed ampule which was purged with a nitrogen flow for 60 s. The desired volume of deoxygenated stock solution of monomer and Mohr's salt (50 mL) was transferred into the ampule without contact with air by using a syringe and needle. NIPAM polymerization was therefore initiated by the redox decomposition of peroxides, and allowed to proceed under vigorous stirring at a temperature of 27 ºC or 50 ºC, with monomer concentrations ranging from 0.1 M to 1.0 M and reaction time up to 300 min. The reaction was stopped by equilibrating the reaction vessel open in contact with air at ambient temperature. The purification of grafted MCC was carried out by centrifugation at 10,000 rpm for 15 min. The isolated precipitate was redispersed in pure water under stirring for 30 min, and subject to centrifugation and filtration. The purification cycle was repeated three times to ensure the total elimination of ungrafted NIPAM homopolymer. The sediment isolated from the ultimate purification stem was dried in an oven at 40 °C to constant weight.

Elemental Analysis

The mass content in C, H and N was determined by elemental analysis a Thermo FLASHER 1112 series equipement calibrated with 2,5-bis(tert-butyl-benzoxazole-2-yl)thiophene and

sulfanilamide as standards. Unmodified cellulose material as well as poly(NIPAM)-grafted cellulose were oven-dried at 60°C for 1 day before analysis. Duplicate measurements were performed for each sample. The reported data are the corresponding average values.

Characterization by Fourier-Transform Infrared Spectroscopy (FTIR)

Oven-dried samples of unmodified MCC, MCC-grafted poly(NIPAM), and poly(NIPAM), were incorporated with dry KBr powder (200 mg) to obtain a concentration of approximately 1 wt-%. The two solids were carefully mixed and pressed to form disk-shaped pellets. Mid-infrared spectra were recorded in transmission mode on a Nicolet FTIR spectrometer by accumulating 32 scans with a resolution of 4 cm^{-1}.

Crystallinity of cellulosic materials

The degree of crystallinity of initial and poly(NIPAM)-grafted materials was determined on oven-dried samples using an X-ray powder diffractometer (PANalytical, X'Pert PRO MPD PW 3040/60) operating with Ni-filtered Cu Kα radiation (λ = 0.15418 nm). Diffraction data was collected at 50 kV and 120 mA. Each sample was scanned nine times with 2θ values ranging from 10° to 50°. The crystallinity index (χ_c) of unmodified and MCC-grafted poly(NIPAM) was calculated using the Segal equation (Park et al., 2010):

$$X_c = \frac{I_{200} - I_{am}}{I_{200}} \times 100\% \qquad \text{Equation 1}$$

where I_{200} is the maximum intensity of the peak maximum at a 2θ value of 22.7°, and I_{am} represents the intensity of the baseline at 2θ value of about 18.0 °.

Imaging of Materials by Scanning Electron Microscopy

The surface morphology of unmodified MCC and poly(NIPAM)-grafted MCC was examined using a Field Emission Scanning Electron Microscopy (FESEM) by Zeiss Supra 55VP model, equipped with energy-dispersive X-ray spectrometry (EDX). All samples were dried

and outgassed prior to sputter-coating with platinum, and then analysed at an accelerating voltage of 2 kV in low vacuum mode.

Energy Dispersive X-ray Spectroscopy (EDX)

Elemental composition of the surface of unmodified and poly(NIPAM)-grafted MCC samples was performed on a CLEO 1455 VP – SEM Energy-dispersive X-ray spectrometer fitted on the SEM for mapping the surface of the samples.

Thermogravimetric analyses

Thermogravimetric analysis (TGA) was performed on oven-dried samples of unmodified cellulosic starting materials, poly(NIPAM)-grafted MCC, and poly(NIPAM) was performed on a thermal analyzer from TA Instruments (TGA 2950) under nitrogen flow. Samples of ca. 10 mg were heated up to 600 ºC at a heating rate of 5 ºC min^{-1}.

Application of the pre-irradiation peroxidation and graft polymerization protocol to cellulose nanocrystals (CNC)

A measured volume of irradiated CNC suspension (10 mL) was transferred into an ampule and closed tightly for purging with gaseous N_2 to ensure an inert atmosphere. In another closed beaker, 1.0 M NIPAM solution with 0. 4 mM Mohr's salt was prepared and purged with under N_2 flow for 10 minutes. The deoxygenated monomer solution (10 mL) was then transferred to the ampule containing the CNC suspension to perform graft polymerization. The reaction took place in a water bath at 27 ºC under continuous stirring. After 60 min, the ampule was opened in the air to stop the reaction. The grafted CNCs were purified by doing 3 cycles of centrifugation (10k rpm, 20 min), then the CNC suspension was mixed with 30 mL of ultrapure water and transferred to dialysis tube (membrane cut-off 12-14 kDa). Dialysis was continued for 3 days, the water changes 3 times per day. After grafting, the dried modified CNS were easily redispersed in cold ultrapure water to the desired concentration.

Turbidimetry

The turbidity of unmodified and grafted CNC suspensions in water was determined by measuring the transmittance with a Cary 50 UV-visible spectromer equipped with a thermally regulated cell holder. The samples were diluted to 0.1 % in ultrapure water and placed in 1 cm-long suprasil cuvette. Transmittance measurements were performed from 400 to 900 nm at temperatures ranging from 25 ºC to 55 ºC with a 2°C interval. The samples were maintained for 5 minutes at the measurement temperature to allow equilibration before recording the transmittance. A cooling ramp from 55°C to 25°C was then applied in the same conditions for evaluating the reverse process.

Result and Discussion

Preliminary tests confirmed the anticipated merit of the peroxidation method (Scheme 2) in comparison with the simultaneous method performed by 10 MeV EB-irradiation of MCC immerged in N_2-saturated aqueous monomer solutions (0.1 - 1 M of NIPAM, and 0.4 M Mohr's salt) at doses between 10 and 50 kGy (Mohamad, 2019). In the conditions we used (see Experimental section) the simultaneous or grafting method produced large amounts of homopolymer which increased the viscosity of the liquid phase, which alters the conditions on graft-polymerization from the surface. After modification, the MCC particles were still isolated and well-dispersable in aqueous media, likely as a consequence of favorable steric repulsion. However, the presence of homopolymers induces risks of pollution of the grafted material by adsorption on the substrates, and reduces the efficiency of the purification step.

The pre-irradiation procedure allowed for better control over reaction temperature, smoother initiation from the substrate's surface and higher uniformity of composition for the reaction medium under continuous stirring. All these factors seemed to be favorable in terms of grafting efficiency measured after extensive purification from unreacted monomer and ungrafted polymer (homopolymer).

NIPAM graft-polymerization from peroxidized MCC

A more sytematic study of essential experimental parameters was therefore conducted to define a proper set of conditions. MCC samples were irradiated with the 10 MeV electron beam accelerator in the presence of air, at doses of 10 and 50 kGy. As a result, free radicals formed at the surface of the particles and in the amorphous zones in contact to oxygen rapidly react to form peroxides or hydroperoxides.

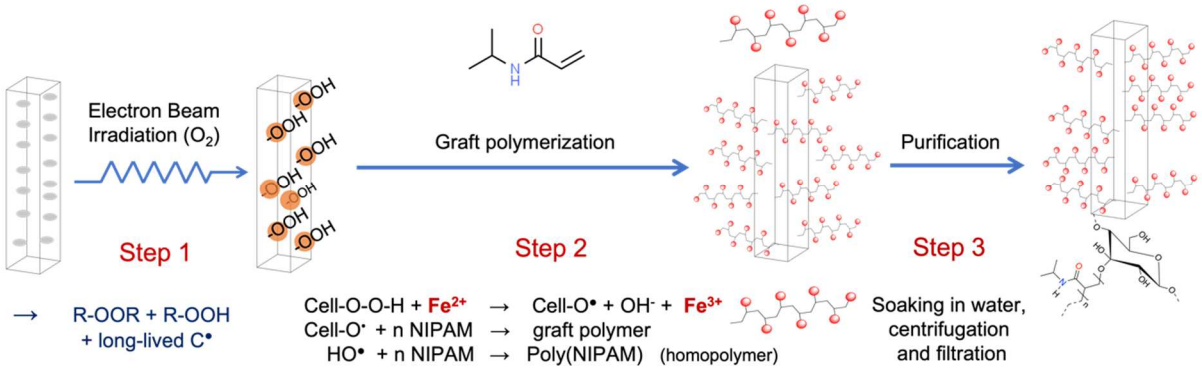

Scheme 2. Sketch representing the three steps NIPAM graft polymerization methods using electron beam pre-irradiation.

After irradiation, the samples were stored at -50°C to limit the thermal decomposition of peroxides. The test experiments were performed with 0.5 g of MCC peroxidized after treatment at various doses. The overall number of anhydroglucose units (AGU) present in the test samples was approximately 3 mmoles. The amount of Mohr's salt present in each grafting solution was set constant to 20 µmoles, whereas NIPAM was introduced in various quantities, between 5 and 50 mmoles in the 50 mL grafting solution. Assuming that the number of peroxides and free radicals present in the irradiated MCC substrates are at least two orders of magnitute lower than the number of AGUs, the mole ratios between these reagents would be comparable with those of free radical polymerization conducted in aqueous media with the Fenton's reagent (Brockway and Moser, 1963; Ferguson and Eboatu, 1989).

We planned to perform grafting reactions at different temperatures, a parameter which may have a complex influence on the course of the chemical modification. Firstly, the redox decomposition of peroxides is thermally activated (Aygun et al., 2012), at least up to temperatures of 40-50°C, inducing

faster reactions mediated by the produced HO• radicals. The mobility around the C-centered radicals occluded within the crystalline domains of MCC can also increase by combined effects of temperature and hydration, hence increasing the number of initiation sites on the substrate. Once polymerization has generated poly(NIPAM) macromolecules as grafts or as free homopolymer, the LCST behavior at temperatures above 32°C, would result in the collapse of Pol(NIPAM) chains on the cellulosic substrate and on the formation of poly(NIPAM) aggregates in the aqueous medium.

The grafting experiments were thus conducted on substrates peroxidized at 2 irradiation doses, reacted at 2 temperatures, 27 and 50°C, with 3 values for the initial content in NIPAM (Fig.1). The upper limit for the irradiation dose was set to 50 kGy to avoid important chain scission on MCC and to maintain its structural properties (Henniges et al., 2012; Polvi et al., 2012), while the lowest dose was selected from the sufficient irradiation dose to initiate graft polymerization with acceptable accuracy on the dose and on its effects on the substrate. The gradual increase of the amount of grafted poly(NIPAM) was monitored for each reaction condition for 4 reactions times, up to 2 or 4 h, for Fig. 1 a-c and Fig. 1-d, respectively.

Determination of the amount of grafted poly(NIPAM) by elemental analysis

The amount of polyNIPAM grafted onto MCC substrate was determined by elemental analysis after extensive purification. To eliminate unreacted monomers, residual Fenton's reagent and homopolymer, the raw products were treated by an iterative purification preocedure. The purified MCC-grafted polyNIPAM was then dried for further analysis. The absence of nitrogen in MCC was confirmed from elemental analysis of the untreated substrate, whereas it is maesured above the detection threshold for grafted MCC samples (Table 1).

Since nitrogen element in the grafted samples can only originate from poly(NIPAM) with a single N atom per N-isopropyl acrylamide unit the wt-fraction of poly(NIPAM) can be calculated from the centesimal content in N atom, using equation 2, where numerical factors, 113.6 and 14

correspond to the rounded values of molecular weight of the NIPAM unit and the mass of 1 mole of N atoms, respectively.

$$Poly(NIPAM)\ content\ (wt\text{-}\%) = N\ content\ (wt\text{-}\%) \times \frac{113.6}{14} \qquad \text{Equation 2}$$

Table 1 - Elemental composition of the starting MCC material and of a selection of isolated poly(NIPAM)-grafted MCC [a] obtained under various experimental conditions.

Sample	[NIPAM] concentration	Reaction time and temperature	Elemental composition			Poly(NIPAM) amount (wt-%)
			Carbon (wt-%)	Hydrogen (wt-%)	Nitrogen (wt-%)	
Unmodified MCC	-	-	42.1	6.4	0.0	0
Grafted MCC	1 M	60 min – 27°C	51.0	8.0	5.9	47.7
Grafted MCC	1 M	120 min – 27°C	51.0	8.1	7.8	63.0
Grafted MCC	1 M	180 min – 27°C	49.0	7.4	6.9	55.6
Grafted MCC	1 M	240 min – 27°C	56.3	8.8	8.8	71.1
Grafted MCC	1 M	60 min – 50°C	51.0	8.0	6.0	48.5
Grafted MCC	1 M	120 min – 50°C	49.0	8.1	5.7	46.1
Grafted MCC	1 M	180 min – 50°C	52.8	7.4	4.7	38.0
Grafted MCC	1 M	240 min – 50°C	44.1	8.8	6.6	53.3
Grafted MCC	0.1 M	30 min – 27°C	42.3	6.5	0.0	0
Grafted MCC	0.1 M	60 min – 27°C	44.9	6.7	0.4	3.2
Grafted MCC	0.1 M	90 min – 27°C	46.9	7.2	0.3	2.4
Grafted MCC	0.1 M	120 min – 27°C	42.8	6.73	0.4	3.2

[a] Peroxidized MMC (0.5 g) after 50 kGy irradiation; $[Fe^{2+}]_0$ = 0.4 mM; total solution volume 50 mL.

Influence of reaction parameters on the extent of grafting

The calculated amounts of grafted poly(NIPAM) were used to correlate the extent of grafting to the tested experimental conditions, as shown in the collected results of Fig. 1.

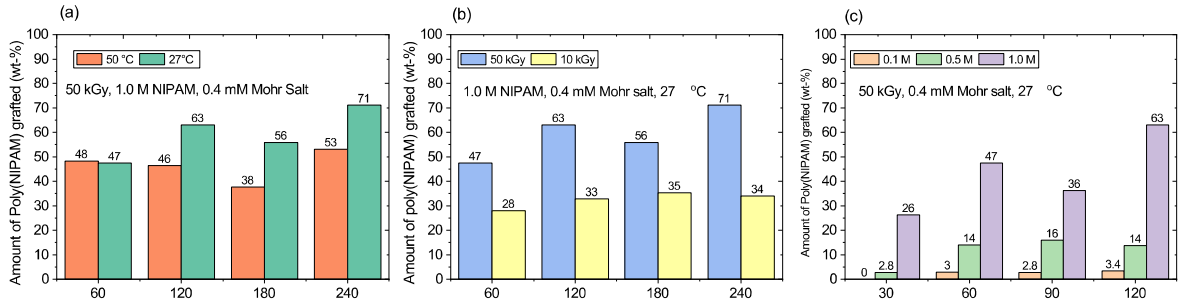

Fig. 1 - Effect of grafting reaction parameters on the amount of grafted poly(NIPAM) on MCC for various durations: reaction temperature of 27 or 50°C for a MCC substrate irradiated at 50 kGy and 1 M initial concentration in NIPAM (a), absorbed dose of radiation (10 or 50 kGy) for grafting at 27°C in presence of 1 M NIPAM concentration (b), and NIPAM concentration (0.1, 0.5 and 1 M) after grafting at 27°C of a MCC substrate irradiated at 50 kGy (c).

A first observation of importance appears from the overall results. For a given set of conditions, the variations due to an increase in reaction time higher than 60 min are lower than the variations measured by changing the initial composition of the reaction mixture. Among the 28 tests along a 2 to 4 h-long grafting process, longer reaction times induced a slight but measurable increase in poly(NIPAM) content. This was not observed only in two particular experiments (Fig. 1-a, time = 180 min) which might have been affected by an uncontrolled factor leading to smaller grafting efficiencies, yet not too much away from the general trend. We can conclude that grafting essentially takes place at very beginning of the reaction. This might be due to a rapid depletion in peroxides at the surface or to the saturation of the surface rendering the grafting process less efficient after a critical value (Sha et al., 2014).

The bar graph of Fig. 1-a shows the amount of grafted poly(NIPAM) in modified MCC along a reaction conducted at 27 or 50°C, for a MCC substrate pre-irradiated at 50 kGy and placed in a 1 MNIPAM solution. We can see that the extent of grafting are almost identical at shorter reaction times. At longer times, the increase in graft polymer is limited, but seems higher for the reaction contacted below the critical temperature. This may be explained by the anticipated collapse of grafted chains at the higher temperature (Gil and Hudson, 2004). This

likely forms a barrier isolating the aqueous monomer solution from the peroxides and free present in the MCC.

With respect to the dose effect on MCC peroxidation, we can see from Fig. 1-b that increasing the dose from 10 to 50 kGy typically enhances the amount of grafted poly(NIPAM) by a factor comprised between 1.5 and 2.1 It is interesting to note here that a rather small dose in terms of polymer processing (10 kGy) allows for the formation of significant levels of surface grafts, while limiting the risks of degradation for the substrate.

Finally, the effect of monomer concentration on the amount of grafted poly(NIPAM) is presented in Fig. 1-c for a substrate peroxidized at 50 kGy and a grafting temperature of 27 ºC. Three levels of concentration were studied with high (1.0 M), medium (0.5 M) and low (0.1 M) NIPAM concentration as a function of reaction time-, for a constant content of Mohr's salt (0.4 mM).

FTIR spectrometry analysis

The MCC-grafted polyNIPAM were characterized by FTIR spectroscopy to identify the spectroscopic signature of the poly(NIPAM) grafts (Fig. 2). For the purpose of comparison, unmodified MCC samples show a strong absorption band at 3350 cm^{-1}, which corresponds to the O-H stretching-mode, a smaller one at 2899 cm^{-1} for the C-H from the methine and methylene groups of glucose units, and while absorbed water and some C=O vibration are responsible for the band at 1645 cm^{-1}. C-O and C-C vibration can see at peaks 1080 and 1043 cm^{-1}. This pattern is typical for cellulose fingerprint in the mid infrared spectral domain (Cichosz and Masek, 2020). Four characteristic groups of new bands are observed in the spectrum of poly(NIPAM)-grafted MCC (Fig. 2). A broad absorption centered at 3080 cm^{-1} corresponds to the N-H stretching of a secondary amide which overlaps the O-H elongation band from the cellulose substrate, the strong asymmetric C-H stretching from methyl groups

(2970 cm^{-1}) and weaker C-H symmetric stretching (2874 cm-1), the amide I and II bands at 1637 and 1519 cm^{-1}, respectively, and the N-H bending band at 1520 cm^{-1}. These peaks were also observed in the spectrum of poly(NIPAM) spectra recorded in the same conditions, confirming its presence on the cellulosic substrate (Shah et al., 2013; Gobeze et al. 2020).

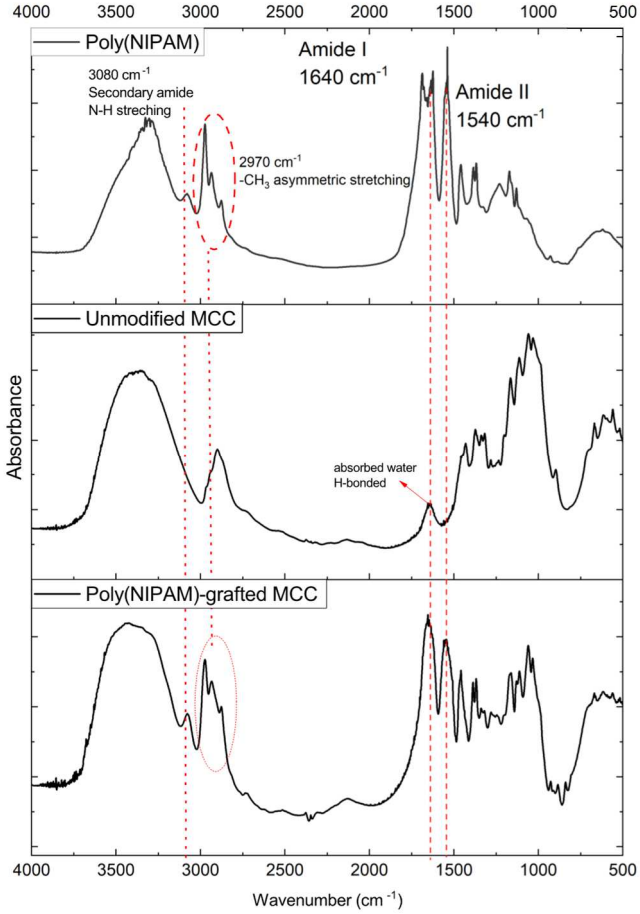

Fig. 2 – Transmission FTIR spectra of poly(NIPAM) (top), unmodified MCC (middle) and poly(NIPAM)-grafted MCC with poly(NIPAM) content of 63 wt-%, all analyzed in KBr pellets.

Influence of pre-irradiation and grafting on the crystal structure of MCC

The analysis by X-ray powder diffraction was performed at first to observe the changes in the crystal structure resulting from the radiation treatment applied before the grafting process and those due to the graft polymerization itself. A semi-quantitative assessment was based on the degree of crystallinity.

The diffractograms presented in Fig. 3-a for an untreated MCC and for samples treated in a slightly hydrated state (equilibrated at 45-50 % relative humidity) with doses of EB radiation ranging from 20 to 100 kGy show very similar diffraction patterns with peaks at 14 °, 16° and 22° corresponding to $(1\,1\,1)$, $(1\,\bar{1}\,0)$ and $(0\,0\,2)$ crystallographic planes, respectively. The three peaks attributed to the presence of different allomorphs of cellulose (Nishiyama et al., 2002). The crystallinity index was calculated from each diffractogram using a method based on the measurement of of peak heights (Park et al., 2010).

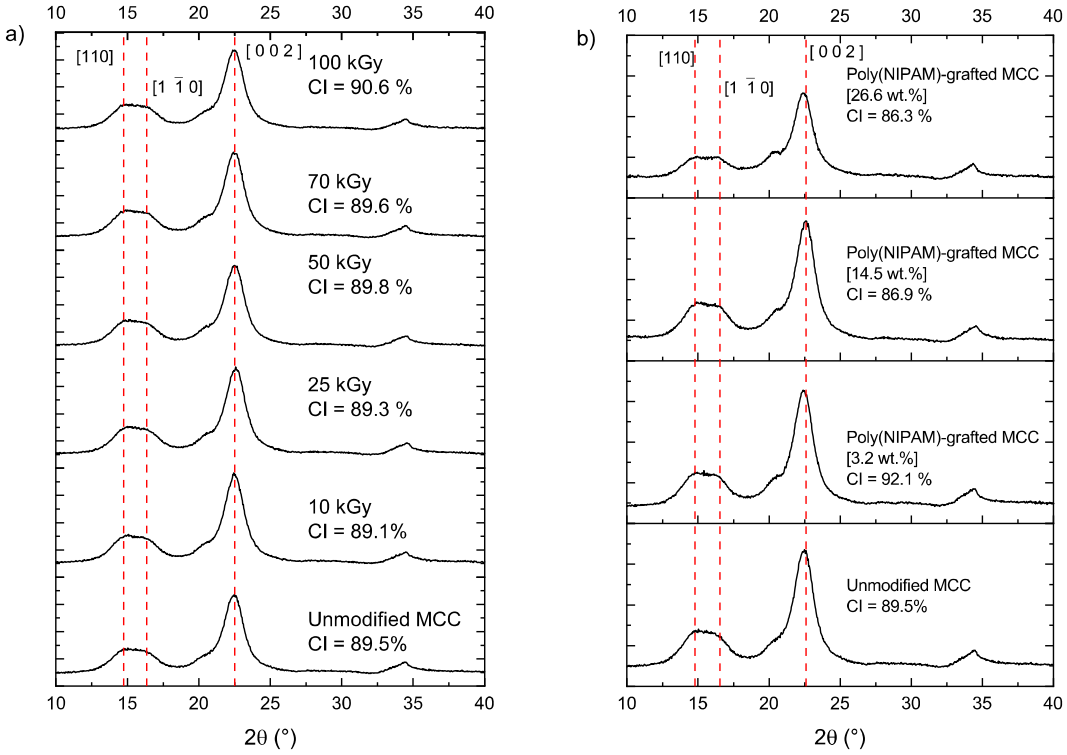

Fig. 3 – X-Ray diffractograms recorded from powder samples of MCC irradiated under EB in solid state for doses ranging from 0 to 100 kGy (a), isolated poly(NIPAM)-grafted MCC with poly(NIPAM) content between 3.2 and 26.6 wt-% (b).

The calculations do not reveal any significant effect resulting from the radiation treatment. After grafting, the effects of the chemical modification of MMC structure as well as the presence of amorphous poly(NIPAM) grafts were evaluated using three different samples with distinct amounts of graft polymer (3.2, 14.5 and 26.2 wt-%, starting from a sbustrate peroxidized with a 50 kGy dose. The diffractograms shown in Fig. 3-b and the corresponding

crystallinity indices indicate a slight decrease of crystallinity when the amount of grafted poly(NIPAM) increases (CI varying from 89.5 to 87 %) for the 2 higher levels of grafting, whereas the sample with very low poly(NIPAM) content apparently shows a higher crystallinity, but the diffrences may not be significant. The slight decrease in crystallinity can be mainly explained for higher poly(NIPAM) contents, by the amorphous nature of the grafts which contribute to the halo under the diffraction pattern. We conclude that the radiation-induced preatreatment and subsequent grafting modification do not significantly affect the crystallinity of the core cellulosic substrate.

Surface morphology

The surface morphology of MCC before and after graft polymerization was observed by field emission scanning electron microscopy coupled with energy dispersive x-ray diffraction (EDX). MCC-grafted polyNIPAM with 77.8 wt. % was used to compare it with unmodified MCC, as shown in Fig. 4. SEM micrograph of a sample of MCC reveals the very rugged surface of the original cellulosic substrate. After grafting, we clearly see that the valleys have been filled and that peaks are smoother, yet showing the typical background structure of the original topographic profile. This accounts for the rather high content in grafted poly(NIPAM).

The EDX spectra reproduced at the bottom of Fig. 4 for modified MCC samples confirmed the presence of nitrogen together with carbon and oxygen. Integration of EDX mapping provides an estimate the average nitrogen content on the surface of grafted MCC and to compare it with carbon and oxygen atoms (data in Fig. 4). The nitrogen content determined by EDX was approximately twice as low as the value measured by elemental analysis (9.4 wt-%), yet well present in the analyzed sample. This may be due to local variations on the amount of graft chains. The distribution of carbon and oxygen however showed a similar pattern while nitrogen mapping appears also quite uniformly present on the surface.

Thermogravimetric analysis

Thermogravimetric analysis (TGA) was performed under nitrogen flow to compare the thermal stability of a modified MCC sample containing 37 wt-% of grafted poly(NIPAM) to the basic constituants, commercial poly(NIPAM) and MCC. The recorded thermograms together with the corresponding derivative plots are shown in Fig. 5.

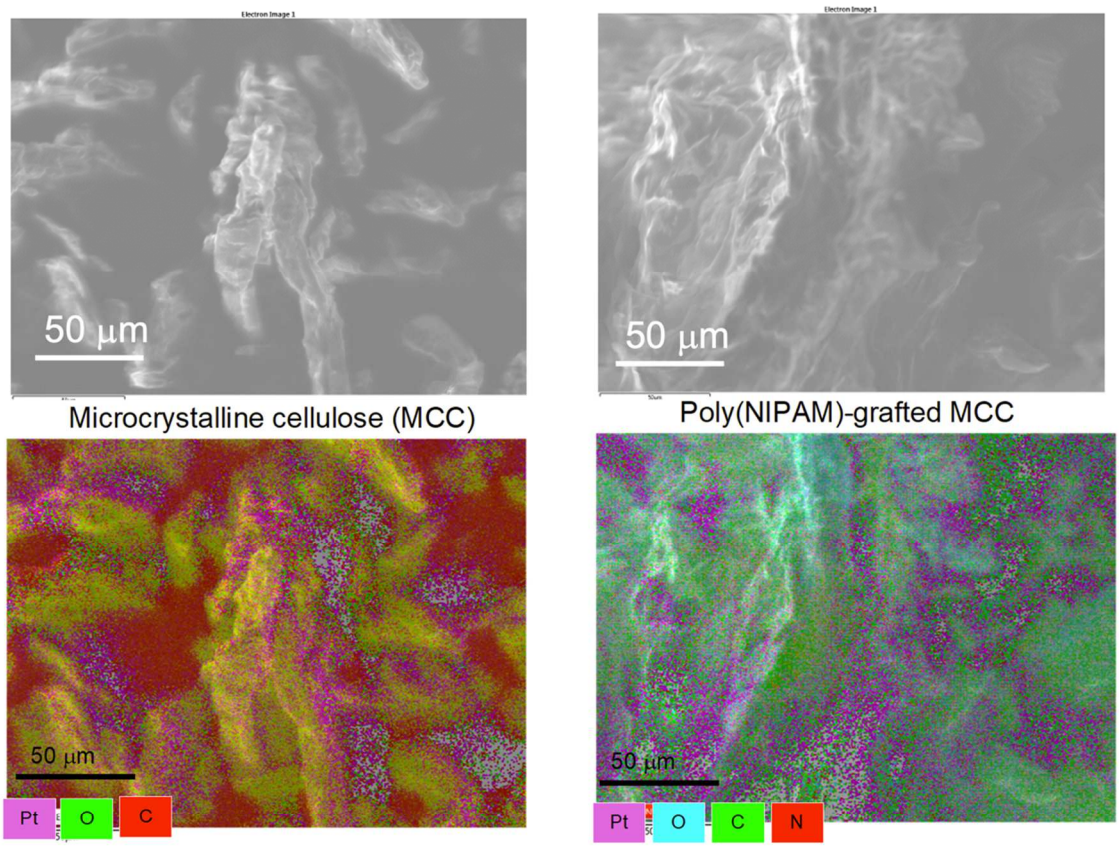

	Atom composition (wt-%)		
Samples	Carbon	Oxygen	Nitrogen
Microcrystalline cellulose (MCC)	54.4	41.9	0
Poly(NIPAM)-grafted MCC	59.2	30	3.8

Fig. 4. SEM micrographs (top) and EDX mapping of element composition for N, C, and O atoms (bottom) on the surface of unmodified MCC (left) and grafted MCC with a poly(NIPAM) content of 77.8 wt-% (right).

Poly(NIPAM) was found to be thermally more stable than the two other materials, showing a maximum decomposition rate at a temperature of 426 ºC, while MCC was comparatively the least thermally stable, with an onset temperature for degradation at 319 ºC. Poly(NIPAM) and MCC, as homopolymers, present a single and monotonous degradation profile as a function of temperature. Poly(NIPAM) degrades extensively, without significant pyrolytic residue at 500°C. The 2 materials containing cellulose yield a residue representing 10 ± 2 % of the original sample at this temperature. This is probably due to the propensity of cellulose materials to form carbonaceous materials by pyrolysis under non-oxidative conditions.

Interestingly, the modified MCC with 37 wt-% of poly(NIPAM) exhibits a hybride degradation profile which is undestandable on the basis of the composition in the constituants. The characteristic temperature maximum of each stage of the grafted MCC does not correspond to the one observed in derivative plots of the pure constituents. This feature supports the existence of close molecular interactions between the components in the grafted materials. The shift observed in our system is even greater than the one reported for similar systems composed of cellulose and poly(NIPAM) (Zeinali et al., 2018; Zoppe et al., 2010).

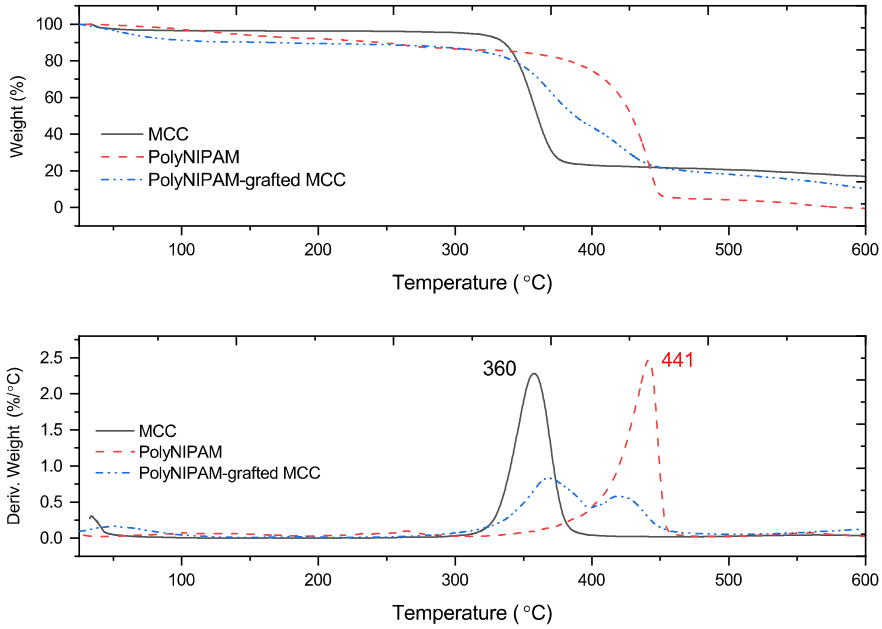

Fig. 5. Thermogravimetric curve of the weight loss and its derivative plot for unmodified MCC, Poly(NIPAM), and poly(NIPAM)-grafted MCC samples (37 wt-% of poly(NIPAM)).

Radiation-induced peroxidation and graft polymerization of NIPAM onto CNCs

We have used CNCs prepared from ramie fibres using the protocol established previously (Hambardzumyan et al., 2012). The basic modification protocol described in the previous sections for MCC modification was tentatively applied to freeze-dried CNCs. The peroxidation stage is easily achieved but it was impossible to redisperse the dry material to obtain a suspension of individual nanoparticles. We have therefore considered the option to

perform the peroxidation on the aqueous suspension. We report here our preliminary results obtained from suspensions with 1.0 wt-% CNCs submitted to 10 kGy irradiation in the presence of oxygen. The irradiated CNC sample were then used for graft polymerization.

The reaction was carried out for CNCs using 1.0 M of NIPAM reacted at 27 °C under nitrogen atmosphere for 60 min. Then, the CNCs suspension was purified by centrifugation and dialyzed for three days. Elemental analysis allowed to determine the nitrogen content and to deduce the fraction of poly(NIPAM) in the isolated grafted CNC (Table 2).

Table 2 - Elemental composition of the starting CNC material and after graft-polymerization of NIPAM[a)]

Elemental Composition	Carbon (wt-%)	Hydrogen (wt-%)	Sulfur (wt-%)	Nitrogen (wt-%)	Poly(NIPAM) amount (wt-%)
Unmodified CNC	41.4	6.1	0.9	0	0
Poly(NIPAM)-grafted CNC[a)]	44.1	6.7	0.7	1.9	15.2

[a)] Synthesized by pre-irradiation at 10 kGy, and grafting with 1 M NIPAM solution at 27°C for 60 min.

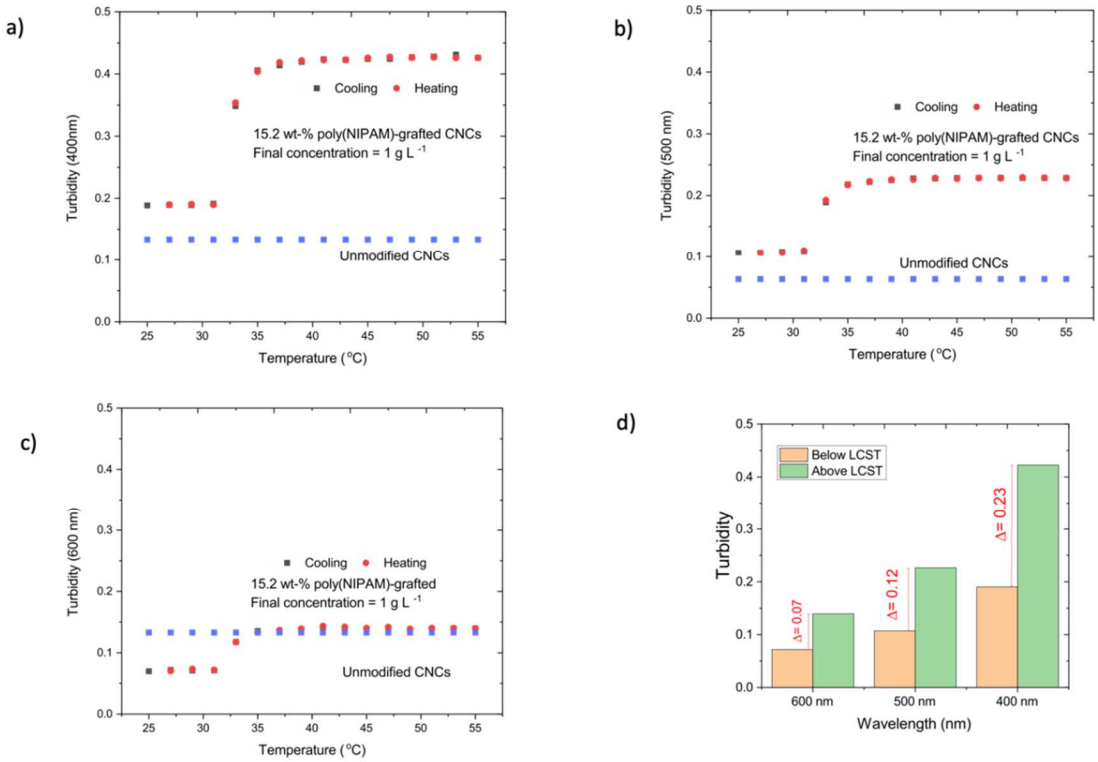

Fig. 6. Temperature-dependance of the turbidity (0.1 wt-% of dry matter in water, 1 cm-optical path)

at 400, 500 and 600 nm of poly(NIPAM)-grafted CNC suspension (15.2 wt-% of poly(NIPAM) content) at temperatures ranging between 25 and 55°C in comparison with the suspension of purified CNCs (graph a-c) and resulting values of the contrast Δ between turbidity values at the 3 wavelengths.

The temperature-reponsiveness of the modified CNC was assessed by turbidimetry in a temperature interval around the critical solution temperature. The unmodified CNC suspension exhibits a low level of turbidity which is independent on temperature in the domain of interest. The presence of sulfate groups originating from the hydrolytic preparation of CNCs catalyzed by sulfuric acid provides electrostatic stabilization via a sufficient density of negative charges. To prepare well-defined characterization protocols in the perspective of our future work focused on CNC modification, we have examined the light scattering properties of the CNC original and modified suspensions at 25 to 55 °C. The turbidity values were measured at three different wavelengths, 400, 500 and 600 nm, during the heating and the cooling. We have defined the constrast at the different wavelengths as the average differences ($\Delta = (\text{Turbidity})_{\lambda,40\text{-}55°C} - (\text{Turbidity})_{\lambda,25\text{-}31°C}$) were calculated at these wavelengths (λ). The turbidity at 400 nm shows the highest contrast value, as shown in Fig. 6-d. The turbidity starts to develop at approximately a temperature of 32 °C to reach a maximum above 50 °C. The milky appearance is due to the aggregation of grafted-CNCs, the behavior being dominated by the loss of hydrophilicity of the poly(NIPAM) grafts. The phase transition observed are reversibly demonstrated from the heating and cooling. Thus, these observations confirm the presence of polyNIPAM grafts at the CNC surface.

Conclusion

The graft polymerization of N-isopropyl acrylamide onto the MCC surface was successfully achieved by radiation-induced graft polymerization. The grafted cellulosic particles were thoroughly purified from unreacted monomer and ungrafted poly(NIPAM) by repeated washing, centrifugation and final filtration. The amount grafted poly(NIPAM) can be

quantified by elemental analysis. The extent of grafting can controlled by irradiation dose, monomer concentration, reaction temperature, and reaction time. Our experiments allow to conclude that graft polymerization proceeds efficiently at 25°C with cellulosic substrates peroxidized by EB-irradiation in the presence of oxygen for doses as low as 10 kGy, while a dose of 50 kGy enhances the extent of grafting without considerable damage to the crystalline structure of MCC. At the concentration of 0.4 mM in ferrous ions, peroxidized MCC initiates efficiently the graft polymerization of NIPAM introduced in concentrations between 0.1 and 1 M in 30 min to 1 h. This allows to conduct the grafting reaction at RT, without need for heating. In such conditions, the collapse on the substrate of grafted poly(NIPAM) chains with LCST properties is avoided. The grafting process can progress until gradual saturation of the substrate's surface by water solvated chains.

Grafting is evidenced by news bands in FTIR, particularly the amide I and amide II fingerprint at 1430 cm^{-1} and 1543 cm^{-1}, respectively. The thermal stability of MCC increased by grafting, and X-ray diffractograms did not reveal a strong decrease of the substrate crystallinity after graft polymerization. SEM micrographs did not show significant changes in the general aspect and morphology of the MCC particles. However, the presence of nitrogen, uniformly distributed over the surface, is observed by EDX, indicating the presence of immobilized and embedded poly(NIPAM) at the particle surface and in the pores.

Based on these results, have applied the pre-irradiation graft polymerization initiated by Fenton reaction to CNCs. To avoid the agreggation of CNC manipulated in a solid and dry state, we have adapted our protocol by using radiation-peroxidized CNCs as aqueous suspensions. The competitive formation of homopolymer initiated by decomposition of hydrogen peroxide generated by the irradiation of aqueous CNC solutions cannot be avoided by this technique, but purification procedures seem satisfactory.

Our future work will aim at the synthesis of poly(NIPAM)-grafted CNCs with varied graft contents and at the study of their basic properties for comparison with similars nanoparticles prepared by more conventional methods (Azzam *et al.* 2016; Zoppe *et al.*, 2010, Du Le et al., 2019). The influence of radiation dose on the crystallinity of the peroxidized nanoparticles should be considered as a specific point of interest, since the nanostructure should be far more sentitive to the defects generated by the direct and indirect effects of radiolysis. The precise quantification of the number of peroxides and hydroperoxide functions on the irradiated cellulosic materials would be very useful to optimize the radiation treatment, to define appropriate storage conditions for their preservation and to control the substrate materials before radiation grafting. We are currently progressing on these different points.

Acknowledgements

The authors thanks Laurence Foulon for the technical support in the preparation of CNCs. The work presented in this article was partially performed in the frame of the IAEA's Coordinated Research Project "Enhancing the Beneficial Effects of Radiation Processing in Nanotechnology". Financial support by CNRS, Conseil Régional, Ministry of Higher Education and Research (MESR) to the PlAneT CPER project is gratefully acknowledged.

References

Aygun, A., Yilmaz, T., Nas, B., Berktay, A., 2012. Effect of temperature on fenton oxidation of young landfill leachate: Kinetic assessment and sludge properties. Glob. Nest J. 14, 487–495. https://doi.org/10.30955/gnj.000835

Azzam, F., Galliot, M., Putaux, J.-L., Heux, L., Jean, B., 2015. Surface peeling of cellulose nanocrystals resulting from periodate oxidation and reductive amination with water-soluble polymers. Cellulose 22, 3701–3714. https://doi.org/10.1007/s10570-015-0785-x

Bhardwaj, Y., Tamada, M., Nho, Y.C., Nasef, M., Güven, O., 2014. Harmonized protocol for radiation grafting. IAEA report,. www-naweb.iaea.org/napc/iachem/working/Graftingprotocol.pdf.

Barsbay, M., Güven, O., 2019. Surface modification of cellulose via conventional and controlled radiation-induced grafting. Radiat. Phys. Chem. https://doi.org/10.1016/j.radphyschem.2019.03.002

Barsbay, M., Güven, O., Stenzel, M.H., Davis, T.P., Barner-Kowollik, C., Barner, L., 2007. Verification of Controlled Grafting of Styrene from Cellulose via Radiation-Induced RAFT Polymerization. Macromolecules 40, 7140–7147. https://doi.org/10.1021/ma070825u

Bhattacharya, A., Misra, B.N., 2004. Grafting: a versatile means to modify polymers: Techniques, factors and applications. Prog. Polym. Sci. 29, 767–814. https://doi.org/http://dx.doi.org/10.1016/j.progpolymsci.2004.05.002

Brockway, C.E., Moser, K.B., 1963. Grafting of poly (methyl methacrylate) to granular corn starch. J. Polym. Sci. Part A Gen. Pap. 1, 1025–1039. https://doi.org/10.1002/pol.1963.100010316

Chapiro A 1962 Radiation Chemistry of Polymeric Systems, Interscience, New York

Cichosz, S., Masek, A., 2020. IR Study on cellulose with the varied moisture contents: Insight into the supramolecular structure. Materials 13, 4573; doi:10.3390/ma13204573

Clochard, M.C., Berthelot, T., Baudin, C., Betz, N., Balanzat, E., Gébel, G., Morin, A., 2010. Ion track grafting: A way of producing low-cost and highly proton conductive membranes for fuel cell applications. J. Power Sources 195, 223–231. https://doi.org/10.1016/j.jpowsour.2009.07.016

Du Le, H., Loveday, S.M., Singh, H., Sarkar, A., 2020. Pickering emulsions stabilised by hydrophobically modified cellulose nanocrystals: Responsiveness to pH and ionic strength. Food Hydrocoll. 99. https://doi.org/10.1016/j.foodhyd.2019.105344

Ershov, B.G., 1998. Radiation-chemical degradation of cellulose and other polysaccharides. Russ. Chem. Rev. 67, 315–334. https://doi.org/10.1070/RC1998v067n04ABEH000379

Ferguson, J., Eboatu, A., 1989. Redox-initiated template polymerization of acrylic acid by means of Fenton's reagent: initiator complexation. Eur. Polym. J. 25, 731–735. https://doi.org/10.1016/0014-3057(89)90038-4

Fu, Z., Gu, X., Hu, L., Li, Y., Li, J., 2020. Radiation induced surface modification of nanoparticles and their dispersion in the polymer matrix. Nanomaterials 10, 1–15. https://doi.org/10.3390/nano10112237.

Garnett, J. L., 1979. Grafting. Radiat. Phys. Chem. **14**, 79-99.

Gil, E.S., Hudson, S.M., 2004. Stimuli-reponsive polymers and their bioconjugates. Prog. Polym. Sci. 29, 1173–1222. https://doi.org/http://dx.doi.org/10.1016/j.progpolymsci.2004.08.003

Gobeze, H.B., Ma, J., Leonik, F.M., Kuroda, D.G., 2020. Bottom-up approach to assess the molecular structure of aqueous poly(N-isopropylacrylamide) at room temperature via infrared spectroscopy. J. Phys. Chem. B 124, 11699–11710. https://doi.org/10.1021/acs.jpcb.0c08424

Guthrie, J. T., 1975. Developments in radiation grafting onto cellulosics. Polymer **16**, 134-150.

Güven, O., 2021. Radiation-Assisted Synthesis of Polymer-Based Nanomaterials. Appl. Sci. 11. https://doi.org/10.3390/app11177913

Hambardzumyan, A., Foulon, L., Chabbert, B., Aguié-Béghin, V., 2012. Natural organic UV-absorbent coatings based on cellulose and lignin: Designed effects on spectroscopic properties. Biomacromolecules. https://doi.org/10.1021/bm301373b

Hao, Y., Peng, J., Li, J., Zhai, M., Wei, G., 2009. An ionic liquid as reaction media for radiation-induced grafting of thermosensitive poly (N-isopropylacrylamide) onto microcrystalline cellulose. Carbohydr. Polym. 77, 779–784. https://doi.org/10.1016/j.carbpol.2009.02.025

Henniges, U., Okubayashi, S., Rosenau, T., Potthast, A., 2012. Irradiation of Cellulosic Pulps: Understanding Its Impact on Cellulose Oxidation. Biomacromolecules 13, 4171–4178. https://doi.org/10.1021/bm3014457

Iller, E., Kukiełka, A., Stupińska, H., Mikołajczyk, W., 2002. Electron-beam stimulation of the reactivity of cellulose pulps for production of derivatives. Radiat. Phys. Chem. 63, 253–257. https://doi.org/http://dx.doi.org/10.1016/S0969-806X(01)00646-6

Kumar, A., Negi, Y.S., Choudhary, V., Bhardwaj, N.K., Singh, Y., Choudhary, V., Kant, N., 2014. Effect of modified cellulose nanocrystals on microstructural and mechanical properties of polyvinyl alcohol/ovalbumin biocomposite scaffolds. Mater. Lett. 129, 61–64. https://doi.org/10.1016/j.matlet.2014.05.038

LeMoigne, N., Sonnier, R., El Hage, R., Rouif, S., 2017. Radiation-induced modifications in natural fibres and their biocomposites: Opportunities for controlled physico-chemical modification pathways? Ind. Crops Prod. 109, 199–213. https://doi.org/10.1016/j.indcrop.2017.08.027

Madrid, J.F., Abad, L. V., 2015. Modification of microcrystalline cellulose by gamma radiation-induced grafting. Radiat. Phys. Chem. 115, 143–147. https://doi.org/10.1016/j.radphyschem.2015.06.025

Mohamad, S. F., 2019. PhD Dissertation, Université de Reims Champagne Ardenne

Nasef, M.M., Güven, O., 2012. Radiation-grafted copolymers for separation and purification purposes: Status, challenges and future directions. Prog. Polym. Sci. 37, 1597–1656. https://doi.org/10.1016/j.progpolymsci.2012.07.004

Othman, S. H., Majid, N., A., Tawakkal, I. S. M. A., Basha, R. K., Nordin, N., Shapii, R. A., 2019. Tapioca starch films reinforced with microcrystalline cellulose for potential food packaging application. Food Sci. Technol., DOI: Dhttps://doi.org/10.1590/fst.36017

Nishiyama, Y., Langan, P., Chanzy, H., 2002. Crystal Structure and Hydrogen-Bonding System in Cellulose Iβ from Synchrotron X-ray and Neutron Fiber Diffraction. J. Am. Chem. Soc. 124, 9074–9082. https://doi.org/10.1021/ja0257319

Park, S., Baker, J.O., Himmel, M.E., Parilla, P.A., Johnson, D.K., 2010. Cellulose crystallinity index: measurement techniques and their impact on interpreting cellulase performance. Biotechnol. Biofuels 3, 10. https://doi.org/10.1186/1754-6834-3-10

Polvi, J., Luukkonen, P., Nordlund, K., Järvi, T.T., Kemper, T.W., Sinnott, S.B., 2012. Primary Radiation Defect Production in Polyethylene and Cellulose. J. Phys. Chem. B 116, 13932–13938. https://doi.org/10.1021/jp309979p

Rodriguez, S. A., Martinez, Ma E.P., Reyes, J.L., 1979. Advances in radiation treatment of natural fibers. Radiat. Phys. Chem. 14, 905–909. https://doi.org/https://doi.org/10.1016/0146-5724(79)90126-2

Seko, N., Tamada, M., Yoshii, F., 2005. Current status of adsorbent for metal ions with radiation grafting and crosslinking techniques. Nucl. Instruments Methods Phys. Res. Sect. B Beam Interact. with Mater. Atoms 236, 21–29. https://doi.org/10.1016/j.nimb.2005.03.244

Sha, X., Xu, X., Sohlberg, K., Loll, P.J., Penn, L.S., 2014. Evidence that three-regime kinetics is inherent to formation of a polymer brush by a grafting-to approach. RSC Adv. 4, 42122–42128. https://doi.org/10.1039/c4ra05663a

Shah, N., Ul-Islam, M., Khattak, W.A., Park, J.K., 2013. Overview of bacterial cellulose composites: A multipurpose advanced material. Carbohydr. Polym. 98, 1585–1598. https://doi.org/10.1016/j.carbpol.2013.08.018

Shahid-ul-Islam, Mohammad, F., 2015. High-Energy Radiation Induced Sustainable Coloration and Functional Finishing of Textile Materials. Ind. Eng. Chem. Res. 54, 3727–3745. https://doi.org/10.1021/acs.iecr.5b00524

Sharif, J., Mohamad, S.F., Fatimah Othman, N.A., Bakaruddin, N.A., Osman, H.N., Güven, O., 2013.

Graft copolymerization of glycidyl methacrylate onto delignified kenaf fibers through pre-irradiation technique. Radiat. Phys. Chem. 91, 125–131. https://doi.org/10.1016/j.radphyschem.2013.05.035

Şolpan, D., Torun, M., Güven, O., 2010. Comparison of pre-irradiation and mutual grafting of 2-chloroacrylonitrile on cellulose by gamma-irradiation. Radiat. Phys. Chem. 79, 250–254. https://doi.org/10.1016/j.radphyschem.2009.09.008

Stannett, V. T., 1990. Radiation grafting : State-of-the-Art. Radiat. Phys. Chem. **35** (1-3), 82-87.

Takács, E., Wojnárovits, L., Borsa, J., Földváry, C., Hargittai, P., Zöld, O., 1999. Effect of γ-irradiation on cotton-cellulose. Radiat. Phys. Chem. 55, 663–666. https://doi.org/10.1016/S0969-806X(99)00245-5

Tataru, G., Guibert, K., Labbe, M., Leger, R., Rouif, S., Coqueret, X., 2020. Modification of flax fiber fabrics by radiation grafting: Application to epoxy thermosets and potentialities for silicone-natural fibers composites. Radiat. Phys. Chem. 170. https://doi.org/10.1016/j.radphyschem.2019.108663

Ulman, K.N., Shukla, S.R., 2016. Admicellar Polymerization and Its Application in Textiles. Adv. Polym. Technol. 35, 307–325. https://doi.org/10.1002/adv.21556

Wojnárovits, L., Földváry, C.M., Takács, E., 2010. Radiation-induced grafting of cellulose for adsorption of hazardous water pollutants: A review. Radiat. Phys. Chem. 79, 848–862. https://doi.org/10.1016/j.radphyschem.2010.02.006

Zeinali, E., Haddadi-Asl, V., Roghani-Mamaqani, H., 2018. Synthesis of dual thermo- and pH-sensitive poly(*N* -isopropylacrylamide- *co* -acrylic acid)-grafted cellulose nanocrystals by reversible addition-fragmentation chain transfer polymerization. J. Biomed. Mater. Res. Part A 106, 231–243. https://doi.org/10.1002/jbm.a.36230

Zoppe, J.O.J.O., Habibi, Y., Rojas, O.J.O.J., Venditti, R.A.R.A., Johansson, L.-S.L.-S., Efimenko, K., Österberg, M., Laine, J., Sterberg, M.O.¨, Laine, J., Osterberg, M., Laine, J., Österberg, M., Laine, J., 2010. Poly(N-isopropylacrylamide) brushes grafted from cellulose nanocrystals via surface-initiated single-electron transfer living radical polymerization. Biomacromolecules 11, 2683–2691. https://doi.org/10.1021/bm100719d